Atomic layer deposition of highly dispersed Pt-nanoparticles on high surface area electrode backbone for electrochemical promotion of catalysis

Y. Hajar[a,1], V. Di Palma[b,1], V. Kyriakou[c], M.A. Verheijen[b], E.A. Baranova[a,d], P. Vernoux[d], W.M.M. Kessels[b], M. Creatore[b], M.C.M. van de Sanden[b,c] M. Tsampas[c,*]

[a]Department of Chemical and Biological Engineering, Centre for Catalysis Research and Innovation, University of Ottawa,161 Louis-Pasteur, Ottawa, ON, K1N 6N5, Canada

[b]Department of Applied Physics, Eindhoven University of Technology, 5600 MB Eindhoven, the Netherlands

[c]Dutch Institute For Fundamental Energy Research (DIFFER), 5612 AJ Eindhoven, the Netherlands

[d]Université de Lyon, Institut de Recherches sur la Catalyse et l'Environnement de Lyon, UMR 5256, CNRS, Université Claude Bernard Lyon 1, 2 avenue A. Einstein, 69626 Villeurbanne, France

[1]First and second authors have contributed equally and possess the first authorship of this article.

*Corresponding author, m.tsampas@differ.nl

Abstract

A novel catalyst design for electrochemical promotion of catalysis (EPOC) is proposed for overcoming the main bottlenecks that limit EPOC commercialization, i.e., low dispersion and surface area of metal catalysts. We have increased surface area by using a porous composite electrode backbone made of $(La_{0.8}Sr_{0.2})_{0.95}MnO_{3-\delta}/Ce_{0.9}Gd_{0.1}O_{1.95}$ (LSM/GDC). Highly dispersed Pt nanoparticles with an average diameter of 6.5 nm have been deposited on LSM/GDC by atomic layer deposition (ALD). This novel design offers, for the first time, a controllable and reproducible way for the fabrication of EPOC catalysts. The performance of the bare electrode backbone shows negligible activity for propane oxidation, while in the presence of Pt-nanoparticles a high catalytic activity is obtained above 200 ^{o}C. The performance of the Pt loaded LSM/GDC catalyst was significantly improved by application of small currents (I < 500 μA), leading to 27-33% increase as a function of the open circuit catalytic rate, with apparent Faradaic efficiency values from 1000 to 3860 % at 300 ^{o}C. Our results point out to EPOC as valid approach to enhance the catalytic activity of nano-structured catalysts.

Keywords: Electrochemical Promotion of Catalysis, Atomic Layer Deposition, Pt-nanoparticles, LSM/GDC composite electrode, Propane oxidation

1 Introduction

The approach of electrochemical promotion of catalysis (EPOC) refers to the pronounced, reversible and controlled changes in catalytic properties (activity and selectivity) upon electrical polarization [1-4]. Since the discovery of the effect [5], more than 100 different catalytic systems have been electrochemically promoted on various metal catalysts supported on different ionic conductors [1-6].

In EPOC studies, an electrochemical cell is employed, in which one of the electrodes is the catalyst for the reaction under study. By controlling the polarization, ions can be pumped to or away from the catalyst, changing its work function and thus its catalytic properties [1-6]. Despite the apparent advantages of this system, such as *in-situ* controlling the coverage of the promoting ions, EPOC has not yet been applied in industry, mainly due to the much lower activity per catalytic mass, than the classic nano-dispersed powders [2,7-12]. Therefore, in the

last few years, EPOC research has been focused on overcoming this issue, which will bring the concept closer to scale-up [2,7-17].

The most promising EPOC catalyst design has been reported by Kambolis et al., in which Pt nanoparticles have been deposited by wet impregnation into the porosity of a LSCF/GDC ($La_{0.6}Sr_{0.4}Co_{0.2}Fe_{0.8}O_{3-\delta}/Ce_{0.9}Gd_{0.1}O_{1.95}$) electrode [10]. This design is inspired by solid oxide electrolyte cells (SOEC) [18] and offers a higher surface area in the porosity of LSCF/GDC than conventional pure metallic films. In addition, LSCF plays mainly the role of electronic conductor and GDC the ionic conductor [19], so their combination provides the two functionalities that are important for electrocatalysis [1-4]. The aforementioned approach has resulted in highly dispersed Pt nanoparticles of 3-20 nm with average size of 8 nm. However, wet impregnation constitutes a poor technique in terms of reproducibility and control of the particle load and its size distribution. Thus, in this study we propose a more reliable deposition method, i.e. atomic layer deposition (ALD) in order to overcome the above limitations.

ALD is a thin film deposition technique based on the chemical reaction of gas phase species on a solid surface. ALD is currently being used commercially by the semiconductor industry and thin-film magnetic head industry. Recently, ALD has raised interest from new application areas, such as photovoltaics and organic electronics. It is performed by the sequential exposure of the substrate to two (or more) different gas species separated in time by purging steps. Each gas species reacts with the substrate up to saturation, through a self-limiting reaction mechanism. Because of its self-limiting nature, the main advantages of ALD are the control of film thickness at atomic scale, high conformity with surface features and high reproducibility [20-26]. On most metal oxides, ALD of a metal generally starts with the growth of small islands (i.e. nanoparticles) and many ALD cycles are required to obtain a film completely closed. Therefore, ALD is ideal for accessing and decorating the entire volume of our porous electrode backbone with Pt-nanoparticles.

Along these lines, the aim of this study is to investigate the electro-promotion of propane oxidation over highly dispersed Pt nanoparticles prepared by ALD. The electrode backbone in which Pt nanoparticles are deposited is a porous $(La_{0.8}Sr_{0.2})_{0.95}MnO_{3-\delta}/Ce_{0.9}Gd_{0.1}O_{1.95}$ (LSM/GDC) composite, which offers mixed ionic-electronic conductivity. 100 Pt ALD cycles were selected based on literature findings of Pt deposition on flat Al_2O_3 substrates where 100 cycles resulted in an average size of 4.5 nm of Pt-nanoparticles [22].

2 Experimental

2.1 Cell preparation and characterization

Two commercial partial cells (FuelCellMaterials) with a 50 μm LSM/GDC composite electrode (50%-50%, 17 mm diameter) deposited on a 150 μm Hionic™ electrolyte support (20 mm diameter) were employed in the present study. One was used as a reference cell, while the second was dedicated to the Pt ALD case study.

Two gold films were deposited on the opposite side of the Hionic™ pellet, in order to act as counter and reference electrodes, respectively. Gold was selected due to its negligible catalytic activity in propane oxidation, as verified through blank experiments under experimental conditions. An electrochemical workstation Voltalab PGP 201 (Radiometer) was used in order to apply and measure both potential and current. The catalyst potential ΔU_{WR} was measured between the working electrode Pt-LSM/GDC and the reference electrode (Au).

ALD of Pt on the porous LSM/GDC was performed using a home-made deposition system described in detail elsewhere [24]. The base pressure of the reactor is $<10^{-6}$ mbar. $MeCpPtMe_3$ (98% from Sigma Aldrich) was used as precursor and O_2 gas at 1 mbar as reactant. The precursor was contained in a stainless steel cylinder, heated at 30 ^oC, and brought into the reactor using Ar as carrier gas. The lines from the precursor to the reactor are heated at 50 ^oC and the reactor wall at 90 ^oC. The ALD recipe starts with 4 s of dosing of $MeCpPtMe_3$, then 3 s of Ar to purge the precursor line and 3 s of pumping down. Then O_2 gas is dosed for 10 s and afterwards the reactor is pumped down for 10 s. The deposition was carried out keeping the substrate holder at 300 ^oC. The ideal Pt ALD deposition on LSM/GDC procedure is shown in Fig.1a.

2.2 SEM and TEM microscopy

A cross-sectional sample for Transmission electron microscopy (TEM) analysis was made by means of standard focus ion beam (FIB) lift-out sample preparation and SEM images by an FEI Nova 600 Nanolab SEM/FIB. Prior to FIB milling a stack of protective layers was deposited in the FIB, consisting of SiO_2 and Pt. Subsequent TEM studies were performed using a JEOL ARM 200 probe corrected TEM, operated at 200 kV, equipped with a 100 mm^2 Centurio SDD EDS detector.

2.3 Catalytic activity measurements

The design of the experimental setup has been described in detail elsewhere [6,13]. The reactant gasses were certified mixtures of 0.80, 5.0 and 99.999% for C_3H_8, O_2 and He (Air Liquide), respectively. Reactants and products analysis was carried out by online gas-chromatography (R3000 micro-GC SRA instruments) and IR spectroscopy (Horiba VA3000).

Under closed circuit, the cell-reactor could operate as an electrochemical oxygen “pump”. Using an external power source, a current, I, can be imposed through the oxygen-ion (O^{2-}) conducting solid electrolyte, which corresponds to an oxygen-ion flux of I/2F. In order to quantify the EPOC, Vayenas and co-workers [1] have defined two dimensionless parameters apparent Faradaic efficiency, Λ, and rate enhancement ratio, ρ, as:

$$\Lambda=(r-r_o)/(I/nF) \quad (1)$$

$$\rho=r/r_o \quad (2)$$

where r is the close-circuit reaction rate (i.e. under polarization) and r_o is the open-circuit reaction rate (i.e. at I = 0) and I/nF is the imposed flux of O^{2-}, where n is the number of exchanged electrons.

3 Results and Discussion

Analysis of Pt-nanoparticles deposited on the porous LSM/GDC is not a trivial task. In our previous work [10] we have employed an extractive replica technique for the TEM analysis of the Pt-nanoparticles, which involves electrode crushing and the dissolution of the electrode backbone in a hydrofluoric acid solution. In order to gain further insight on the Pt-distribution on the electrode backbone, we have conducted a TEM analysis on a cross-section of an electrode (after catalysis). Fig.1b,c illustrates SEM images of the electrode surface before and during FIB preparation of the TEM lamella.

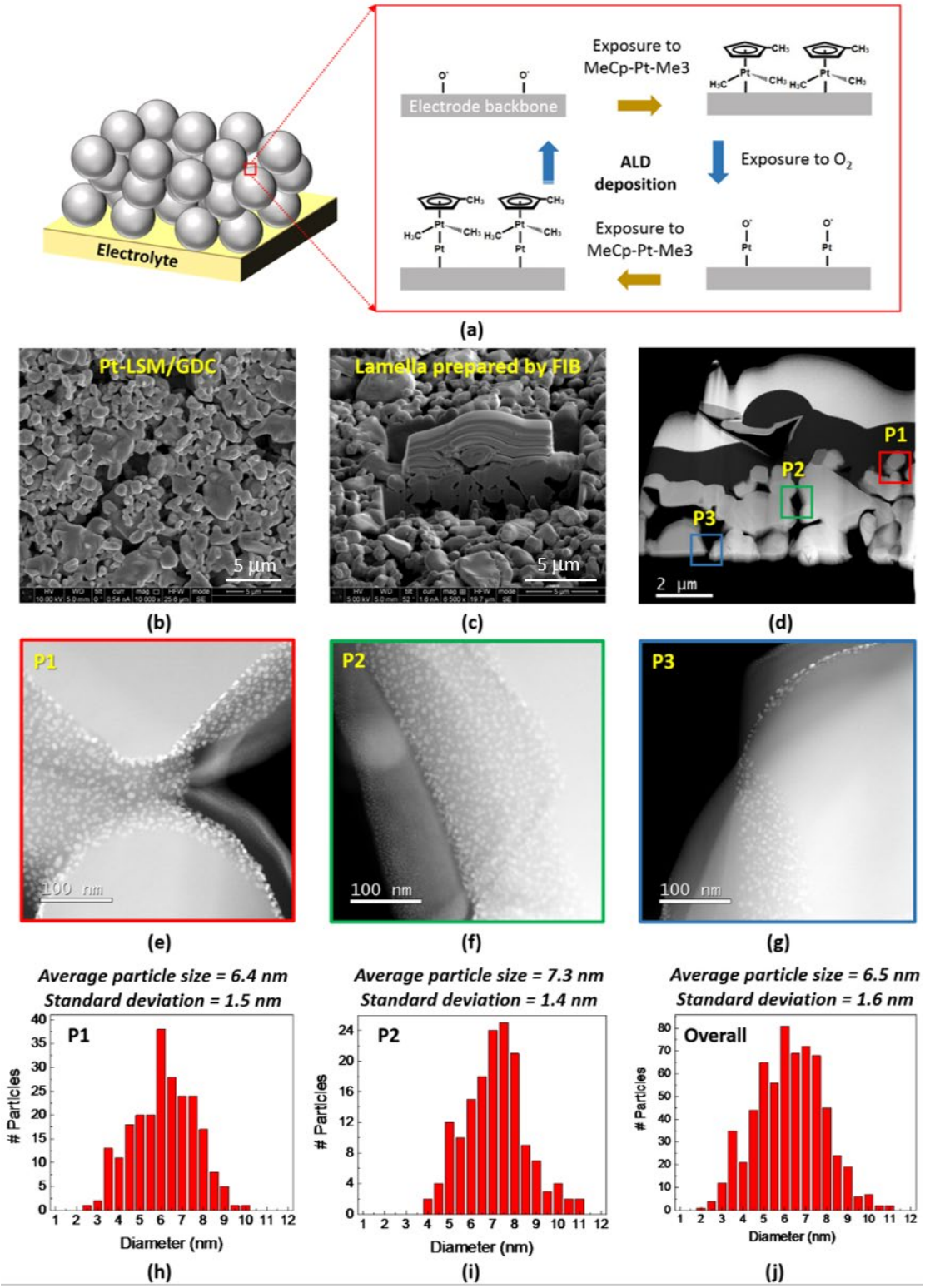

Fig.1 (a) Schematic representation of Pt deposition on the porous-LSM/GDC electrode backbone using ALD. (b) and (c) SEM images of the surface of the Pt loaded LSM/GDC, displaying the location of the cross-section. (d) HAADF-STEM image of the TEM lamella. The sample is covered by a stack of protective SiO_2/Pt layers. (e), (f) and (g) HAADF-STEM images of the Pt loaded LSM/GDC at three different points of interest. (h), (i) and (j) the corresponding size distribution at two points and in the overall lamella.

In Fig.1d a High Angle Annular Dark Field (HAADF)–Scanning TEM image of the entire TEM lamella is displayed. In this sample 3 areas of interest have been denoted as P1, P2 and P3. TEM images of these areas are shown in Fig.1e-g. The presence and distribution of the Pt particles can be clearly discerned. Because of the different inclinations of the grain surfaces with respect to the imaging direction, both vertical as well as lateral dimensions of the Pt particles can be imaged.

The use of ImageJ software allowed for the determination of Pt particle size distribution, which for P1 and P2 areas are presented in Fig.1h,i and for the entire lamella area in Fig.1j. The Pt-nanoparticles have a uniform distribution with a particle size range of 3-10 nm and 6.5 nm average size. Considering hemi-spherical Pt-nanoparticles, one can estimate a Pt-dispersion of 18.2% [27]. Particle size analysis was performed after catalytic evaluation. It is well known that the particle size might increase after catalysis due to agglomeration [28] Moreover, the nanoparticles growth is influenced by the substrate [22]. Taking into account this, the average Pt particle size of 6.5 nm for 100 ALD cycles is not too far from the reported value of 4.5 nm on Al_2O_3 [22].

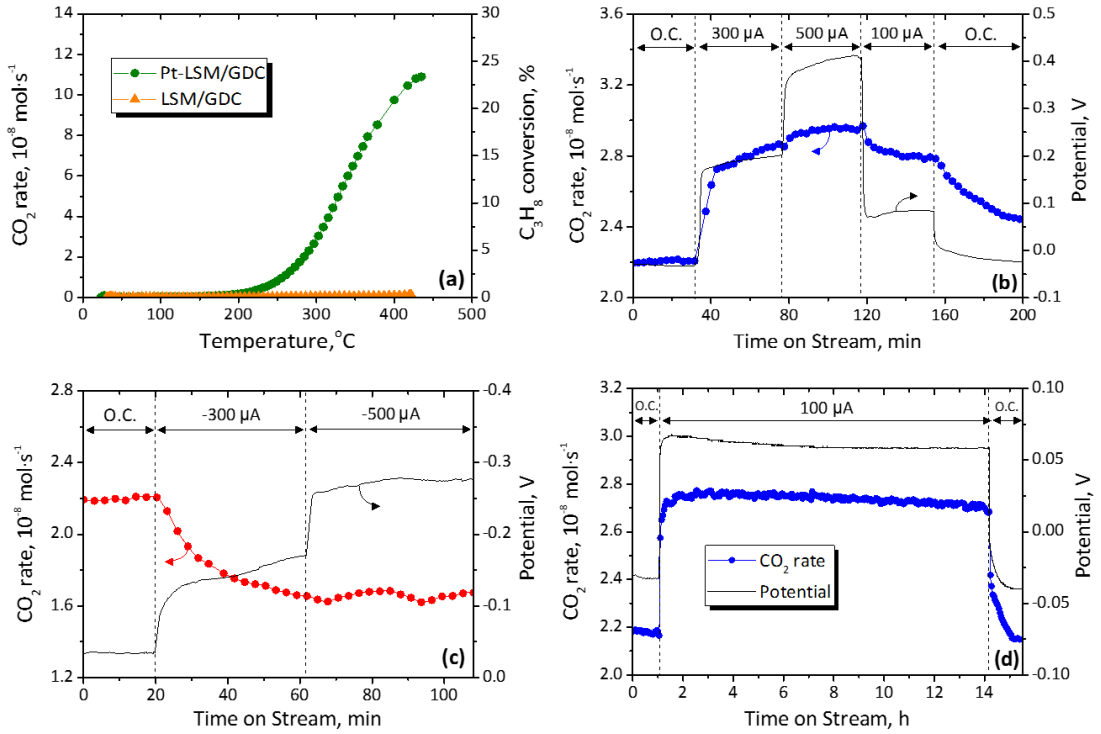

Fig.2 (a) Comparison of catalytic (open-circuit) performance for propane combustion for Pt-LSM/GDC, and bare LSM/GDC support. (b) Effect of positive and (c) negative currents on the potential and CO_2 formation. (d) EPOC stability test under positive polarization. P_{C3H8}/P_{O2} = 0.22 kPa/2.2 kPa, T=300 °C, F_t = 100 ml·min^{-1} (NTP).

In order to evaluate the catalytic performance of Pt-nanoparticles deposited on the LSM/GDC support, light-off experiments were performed on Pt-LSM/GDC (without involving a pre-reduction step for Pt) and bare LSM/GDC samples (Fig.2a). The temperature was increased from ambient to 425 °C with heating rate of 2 °C/min. Fig.2a shows the CO_2 production rate and the C_3H_8 conversion as a function of temperature. It can be seen that the LSM/GDC support was totally inactive for propane oxidation, while the addition of the Pt-nanoparticles

strongly increased the catalytic activity. For the Pt-loaded sample, the conversion of propane was shown to increase rapidly after 200 ^{o}C and reach 23% at 425^{o}C.

The impact of various polarizations between -1.0 V and +1.0 V on the catalytic performance of the Pt-free LSM/GDC sample was investigated at 300°C, in which no modification of the propane conversion was observed. On the other hand, the Pt-loaded LSM/GDC exhibited a non-Faradaic behavior both under positive and negative polarizations. For instance, Fig.2b displays the impact of three consecutive steps of small positive currents (I = 300, 500 and 100 μA) on the catalytic rate of CO_2 production at 300 °C. The rate of propane oxidation gradually increases from 2.20 x 10^{-8} mol $CO_2 \cdot s^{-1}$ and reaches a steady-state value at 2.88, 2.93 and 2.79 x 10^{-8} mol $CO_2 \cdot s^{-1}$, i.e. a rate enhancement of 131, 133 and 127% (ρ = 1.31, 1.33 and 1.27) respectively. The apparent Faradaic efficiency, Λ, was found to be 14.6, 10.0 and 38.6 for the three different applied currents, respectively. Thus, the enhancement of the catalytic activity is up to 38.6 times higher than that predicted by Faraday's law considering an electro-oxidation of propane with oxygen ions. After current interruption the reaction rate returned slowly to its open-circuit value, thus indicating the reversibility of EPOC.

The increase of the reaction rate observed under positive polarization can be explained on the basis of the rules of electrochemical promotion [29]. It has been well-established that the supply of an electronegative ion, such as O^{2-}, to the catalyst-electrode surface, weakens the Pt-O bonds and therefore increases its work function [1-4]. The latter leads to the improved chemisorption of propane, which is known to be linked with the rate-determining step for propane oxidation [30,31]. After current interruption, the $O^{\delta-}$ promoters are consumed and therefore the catalyst returns with time to its initial state [29,30]. The moderate values of the rate enhancement ratio and Faradaic efficiency can be attributed to the pre-activation of the Pt-nanoparticles due to their size via self-driven spillover [1-3]. In addition, only a minor part of the applied current, between the LSM/GDC electrode and the counter electrode, most probably passes across the Pt nanoparticles.

On the other hand, the removal of O^{2-} from the Pt loaded sample (negative current application of -300 and -500 μA) had a poisoning effect on the catalyst, which also resulted in non-faradaic modification on the catalytic rate (Fig.2c) in good agreement with literature [10,29]. Interestingly, the poisoning effect was limited to 74% of the initial reaction rate and a Faradaic efficiency of 12.0. Application of even higher negative current (I = -500 μA) does not change the catalytic rate, this demonstrates a saturation effect, which can be attributed to current bypass from the Pt-nanoparticles. In other words, the higher negative current application cannot affect the performance of Pt-nanoparticles, since the extra current (i.e. oxygen pumping) takes place on Pt-free areas of the LSM/GDC surface.

Finally, the stability of the phenomenon was verified by long-term experiment of 100 μA current application (Fig.2d). The performance of the catalyst is relatively steady since the CO_2 production rate decrease slightly from 2.78 to 2.73 x 10^{-8} mol $CO_2 \cdot s^{-1}$ after 13 h of polarization. This indicates that possible agglomeration of Pt-nanoparticles during the TPO treatment at higher temperature (i.e. 425 ^{o}C) has resulted in a stable catalyst configuration.

4 Conclusions

The combination of ALD with SOEC technological advances led to a Pt decorated composite electrode, which was successfully employed for the electropromotion of propane combustion.

In the implemented design, the three functionalities (i.e. catalytic activity, electronic and ionic conductivity) needed for efficient EPOC catalysts are separated by three phases (i.e. Pt, LSM and GDC). The moderate magnitude of electrochemical promotion can be attributed to the pre-activation of the Pt-nanoparticles due to their small size via self-driven spillover or current by-pass. Future plans for enhancing the magnitude of the effect will be directed in the direction of tuning either the Pt loading and/or the electronic conductivity of the electrode backbone.

Utilization of the ALD technique can bring EPOC systems one step closer to commercialization due to minimized catalyst loadings. In view of practical application of EPOC the success of our concept should be verified with reactions of industrial importance, where possible modifications in product selectivity can also occur.

5 Acknowledgements

Authors acknowledge NWO (NCI-CHIPP.2015.001) programme for partial financial support, B. Barcones for FIB preparation of the TEM sample, Solliance and the Dutch province of Noord-Brabant for funding the TEM facility, doctoral mobility grants (Avenir Lyon Saint-Etienne Program) and iMUST mobility program from Université de Lyon.

6 References

[1] C.G. Vayenas, S. Bebelis, C. Pliangos, S. Brosda, D. Tsiplakides, Electrochemical Activation of Catalysis: Promotion, Electrochemical Promotion and Metal-Support Interactions; Kluwer Academic/Plenum, New York, 2001.

[2] P. Vernoux, L. Lizarraga, M.N. Tsampas, F.M. Sapountzi, A. De Lucas-Consuegra, J.L. Valverde, S. Souentie, C. G. Vayenas, D. Tsiplakides, S. Balomenou, E. A. Baranova, Ionically conducting ceramics as active catalytic supports, Chem. Rev., 113, 10 (2013) 8192-8260.

[3] M.N. Tsampas, F.M. Sapountzi, P. Vernoux, Applications of Yttria Stabilized Zirconia (YSZ) in catalysis, Catal. Sci. Tech., 5 (2015) 4884-4900.

[4] I. Garagounis, V. Kyriakou, C. Anagnostou, V. Bourganis, I. Papachristou, M. Stoukides, Solid electrolytes: applications in heterogeneous catalysis and chemical cogeneration, Ind. Eng. Chem. Res., 50 (2011) 431-472.

[5] M. Stoukides and C. G. Vayenas, The effect of electrochemical oxygen pumping on the rate and selectivity of ethylene oxidation on polycrystalline silver, J. Catal., 70 (1981) 137–146.

[6] M.N. Tsampas, A. Kambolis, E. Obeid, L. Lizzaraga, F. Sapountzi, P. Vernoux, Electrochemical promotion of propane oxidation on Pt deposited on a dense β″-Al_2O_3 ceramic Ag^+ conductor, Front. Chem., 1 (2013) 13.

[7] S. Balomenou, D. Tsiplakides, A. Katsaounis, S. Thiemann-Handler, B. Cramer, G.Foti, Ch. Comninellis, C.G. Vayenas, Novel monolithic electrochemically promoted catalytic reactor for environmentally important reactions, Appl. Catal. B, 52 (3) (2004) 181-196.

[8] C. Xia, M. Hugentobler, Y. Li, C. Comninellis, W. Harbich, Quantifying electrochemical promotion of induced bipolar Pt particles supported on YSZ, Electrochem. Commun., 12 (2010) 1551-1554.

[9] D. Poulidi, M.E. Rivas, I.S. Metcalfe, Controlled spillover in a single catalyst pellet: Rate modification, mechanism and relationship with electrochemical promotion, J. Catal., 281 (2011) 188-197.

[10] A. Kambolis, L. Lizarraga, M.N. Tsampas, L. Burel, M. Rieu, J.-P. Viricelle, P. Vernoux, Electrochemical promotion of catalysis with highly dispersed Pt, Electrochem. Commun., 19 (2012) 5-8.

[11] J. González-Cobos, D. Horwat, J. Ghanbaja, J.L. Valverde, A. de Lucas-Consuegra, Electrochemical activation of Au nanoparticles for the selective partial oxidation of methanol, J. Catal., 317 (2014) 293–302

[12] H.A.E. Dole, L.F. Safady, S. Ntais, M. Couillard, E.A. Baranova, Electrochemically enhanced metal-support interaction of highly dispersed Ru nanoparticles with a CeO_2 support, J. Catal., 318 (2014) 85–94.

[13] Y.M. Hajar, K. D. Patel, U. Tariq, E.A. Baranova, Functional Similarity of Electrochemical Promotion and Metal Support Interaction for Pt and RuO_2 Nanoparticles. J. Catal., 352 (2017) 42-51.

[14] E. Ruiz, D. Cillero, P.J. Martínez, A. Morales, G. San Vicente, G. de Diego, J.M. Sánchez, Electrochemical synthesis of fuels by CO_2 hydrogenation on Cu in a potassium ion conducting membrane reactor at bench scale, Catal. Today., 236 (2014) 108–120.

[15] A. de Lucas-Consuegra, J. González-Cobos, V. Carcelén, C. Magén, J.L. Endrino, J.L. Valverde, Electrochemical promotion of Pt nanoparticles dispersed on a diamond-like carbon matrix. A novel electrocatalytic system for H_2 production, J. Catal., 307 (2013) 18-26.

[16] J. González-Cobos, E. Ruiz-López, J.L. Valverde, A. de Lucas-Consuegra, Electrochemical promotion of a dispersed Ni catalyst for H_2 production via partial oxidation of methanol, Int. J. Hydrog. Energy, 41 (2016) 19418-19429.

[17] V. Roche, R. Revel, P. Vernoux, Electrochemical promotion of YSZ monolith honeycomb for deep oxidation of methane, Catal. Commun., 11 (2010) 1076-1080.

[18] J.T.S. Irvine, D. Neagu, M.C. Verbraeken, C. Chatzichristodoulou, C. Graves, M.B. Mogensen, Evolution of the electrochemical interface in high-temperature fuel cells and electrolysers, Nature Energy, 1, (2016) 15014.

[19] X. Xi, A. Kondo, T. Kozawa, M. Naito, LSCF–GDC composite particles for solid oxide fuel cells cathodes prepared by facile mechanical method, Adv. Powder Technol., 27 (2016) 646-651.

[20] S. M. George, Atomic layer deposition: an overview, Chem. Rev., 110 (2010) 111–131.

[21] C. Detavernier, J. Dendooven, S. P. Sree, K. F. Ludwig and J. A. Martens, Tailoring nanoporous materials by atomic layer deposition, Chem. Soc. Rev., 40 (2011) 5242–5253.

[22] A. J. M. Mackus, M. J. Weber, N. F. W. Thissen, D. Garcia-Alonso, R. H. J. Vervuurt, S. Assali, A. A. Bol, M. A. Verheijen, W. M. M. Kessels, Atomic layer deposition of Pd and Pt nanoparticles for catalysis: on the mechanisms of nanoparticle formation, Nanotechnology, 27 (2016) 034001

[23] J. Lu, J.W. Elam, P.C. Stair, Synthesis and Stabilization of Supported Metal Catalysts by Atomic Layer Deposition, Acc. Chem. Res., 46 (8) (2013) 1806–1815

[24] H.C.M. Knoops, A.J.M. Mackus, M.E. Donder, M.C.M. van de Sanden, P.H.L. Notten, W.M.M. Kessels, ALD of platinum and platinum oxide films, Electrochem. Solid-State Lett., 12 (7) (2009) G34-G36.

[25] C. Marichy, M. Bechelany, and N. Pinna, Atomic Layer Deposition of Nanostructured Materials for Energy and Environmental Applications, Adv. Mater., 24, (2012) 1017–1032.

[26] B. J. O'Neill, D. H. K. Jackson, J. Lee, C. Canlas, P. C. Stair, C. L. Marshall, J. W. Elam, T. F. Kuech, J. A. Dumesic, and G. W. Huber, Catalyst Design with Atomic Layer Deposition, ACS Catal., 5, (2015) 1804−1825.

[27] A. Borodzinski, M. Bonarowska, Relation between Crystallite Size and Dispersion on Supported Metal Catalysts, Langmuir, 13 (1997) 5613-5620.

[28] J. Yang, V. Tschamber, D. Habermacher, F. Garin, P. Gilot, Effect of sintering on the catalytic activity of a Pt based catalyst for CO oxidation: Experiments and modeling, Appl. Catal. B, 83 (3-4) (2008) 229-239.

[29] C.G. Vayenas, S. Brosda, Electron donation–backdonation and the rules of catalytic promotion, Top. Catal., 57, 14-16 (2014) 1287-1301.

[30] M.N. Tsampas, F.M. Sapountzi, A. Boréave and P. Vernoux, Isotopical labeling mechanistic studies of electrochemical promotion of propane combustion on Pt/YSZ, Electrochem. Commun., 26 (2013) 13-16.

[31] L.Lizarraga, M. Guth, A. Billard, P. Vernoux, Electrochemical catalysis for propane combustion using nanometric sputtered-deposited Pt films, Catal. Today, 157 (2010) 61-65.